# Modelling tissue microstructure in bone metastases from prostate cancer using VERDICT MRI

Colleen Bailey[1], Eleftheria Panagiotaki[1], Nina Tunariu[2], Matthew R Orton[3], Veronica A Morgan[3], Thorsten Feiweier[4], David J Hawkes[1], Martin O Leach[3], David J Collins[3], and Daniel C Alexander[1]

*[1]Centre for Medical Image Computing, University College London, London, United Kingdom, [2]Radiology, Royal Marsden NHS Foundation Trust and Institute of Cancer Research, Sutton, United Kingdom, [3]CR-UK and EPSRC Cancer Imaging Centre, Institute of Cancer Research and Royal Marsden NHS Foundation Trust, London, United Kingdom, [4]Healthcare Sector, Siemens AG, Erlangen, Germany*

**INTRODUCTION:** Bone metastases are a major burden in men with advanced prostate cancer. The only imaging criteria available for assessing therapeutic benefit are those of disease progression on bone scans (PCWG) with no imaging criteria defining response[1]; systemic measures such as the PSA blood test may not reflect the response of individual metastases[2]. More functional imaging techniques, such as diffusion MRI combined with biophysical modelling that characterizes microstructure may prove valuable in such cases. We apply a 3-compartment model for diffusion that includes compartments for Vascular, Extracellular and Restricted (intracellular) DIffusion for Cytometry in Tumours (VERDICT). VERDICT has been successfully applied to characterize colorectal cancer xenografts in mouse[3] and clinical prostate cancer data[4]. In this study, we tested VERDICT with different shapes for the vascular and extracellular compartments. We examined these VERDICT models, as well as more conventional 1-, 2- and 3-compartment models that do not incorporate restriction, for goodness and stability of fit and biological relevance.

**METHODS:** Three patients with 7 bone metastases in the pelvis were scanned at 1.5 T (MAGNETOM Avanto, Siemens Healthcare, Germany) using a 24-channel spine matrix coil and 12 channel body matrix coil for receive. Thirteen diffusion-weighted images (DWI; 2D pulsed gradient spin echo, 2.97 x 2.97 $mm^2$, 5 mm thickness, 38 x 38 $cm^2$ field of view, repetition time 3 s, 3 signal averages) were acquired using a research sequence. Each DWI was normalized using an unweighted image of the same echo time (TE) to account for different T2 weightings. Diffusion parameters and TEs are listed in Table 1.

**Table 1** Diffusion scan parameters and echo times

| | | | | | | | | | | | | | |
|---|---|---|---|---|---|---|---|---|---|---|---|---|---|
| Gradient time δ (ms) | 24.8 | 33.2 | 40.0 | 40.2 | 28.2 | 19.0 | 13.4 | 10.0 | 7.4 | 24.8 | 24.8 | 24.8 | 24.8 |
| Diffusion time Δ (ms) | 33.8 | 45.6 | 52.4 | 52.6 | 40.6 | 31.4 | 26.2 | 22.8 | 20.2 | 60.0 | 60.0 | 50.0 | 50.0 |
| b value (s/$mm^2$) | 1000 | 2000 | 3000 | 2500 | 1500 | 800 | 400 | 200 | 100 | 500 | 800 | 800 | 500 |
| TE (ms) | 77.2 | 94.0 | 111.6 | 108.0 | 84.0 | 67.6 | 56.4 | 49.6 | 44.4 | 100.4 | 100.4 | 90.0 | 90.0 |

The models tested and fit parameters for the vascular perfusion (p), intracellular (IC) and extracellular (EC) compartments are summarized in Table 2: Ball (B) = isotropic free diffusion; sphere (S) = isotropic diffusion restricted by an impermeable membrane at radius R; astrosticks (A) restricted diffusion in a set of isotropically oriented cylinders of zero radius. ADC is equivalent to Ball and IVIM to Ball-Ball (BB) in this nomenclature. Diffusion coefficients ($D_x$) were constrained < 2.9 x $10^{-3}$ $mm^2$/s for IC and EC compartments and > 3 x $10^{-3}$ $mm^2$/s for vascular pseudodiffusion. Volume fractions ($f_x$) sum to 1 and R was constrained between 0.1 - 20 µm.

**Table 2** Models tested with fit parameters in parentheses. Total number of fit parameters summarized in the last column

| Model | Vascular | Extracellular | Intracellular | # pars |
|---|---|---|---|---|
| ADC | Ball ($D_{p+EC+IC}$) | | | 1 |
| IVIM | Ball ($f_p$, $D_p$) | Ball ($D_{IC+EC}$) | | 3 |
| BBB | | Ball ($D_{EC}$) | Ball ($f_{IC}$, $D_{IC}$) | 5 |
| BBS | | Ball ($D_{EC}$) | Sphere ($f_{IC}$, $D_{IC}$, R) | 6 |
| BAS | | Astrosticks ($D_{EC}$) | | 6 |
| ABS | Astrosticks ($f_p$, $D_p$) | Ball ($D_{EC}$) | | 6 |

Signal was averaged over a region of interest (ROI) that was confirmed by a radiologist (eg. Fig 1) and fitted using an iterative optimization procedure that accounts for local minima and Rician noise[2,3]. The $\chi^2$ from 1000 fit iterations were examined for model stability. For each model, the minimum objective function from all iterations was selected for comparison using the Akaike Information Criterion (AIC; lower values indicate better fit after adjustment for number of model parameters)[5], and biological feasibility by comparing the model parameters against known features of bone metastases from prostate cancer. In four ROIs where tumour was present in five slices, the standard deviation ($SD_{intratum}$) was calculated across slices.

**RESULTS:** Fits (eg. Fig 2) were stable (>50% fits within 1 standard deviation of the minimum) for ADC, IVIM, BBB and BBS but worse for BAS and ABS. The lowest AIC (Fig 3) was obtained for BBS in 6 ROIs and ABS in 1 ROI although these two models had similarly low AICs in all cases. Parameters (all ROIs) for selected models are summarized in Table 3. For the BAS model, R reached the 20 µm limit allowed by the fitting algorithm.

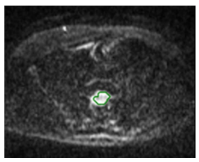

**Figure 1** DWI (b=1000 s/$mm^2$) with bone metastasis selected

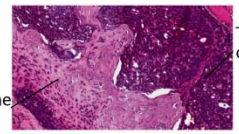


**Figure 4** H&E of bone metastasis model in mouse showing densely-packed tumour cells infiltrating less dense bone matrix.

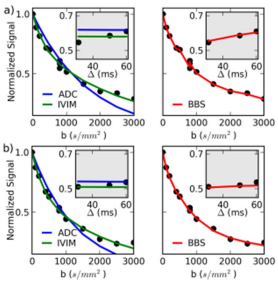


**Figure 2** Fits to selected models for (a) ROI in Fig 1 and (b) an ROI in another patient. Inset shows b=800 s/$mm^2$ points with different Δ.

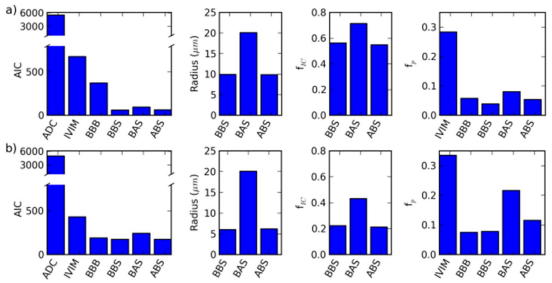


**Figure 3** AIC and selected parameter values for the different models in 2 ROIs (a and b): sphere radius (R), volume fraction of sphere ($f_{IC}$) and perfusive volume fraction ($f_p$).

**DISCUSSION:** The BBS and ABS models had the lowest AICs and provided the best fits to the bone metastasis data, suggesting that diffusion signal in this case can be modelled by three compartments, including a restricted spherical intracellular compartment of radius R and an extracellular compartment with free diffusion. This was true even in cases with low intracellular volume fraction, $f_{IC}$, (Figs. 2b and 3b). The similarity between BBS and ABS fits in spite of different pseudodiffusion compartment shapes (ball and astrosticks) is likely due to the low perfusion fraction, common amongst bone metastases; additional patients may allow these models to be differentiated. Models without a restricted component (ADC, IVIM, BBB) were unable to capture variations in signal with diffusion time, (eg. Fig 2 insets). The BAS model was unstable and provided an estimate of cell radius (20 µm) that was beyond what can be physically measured by the MRI scan parameters, suggesting that astrosticks are a poor model of extracellular space in these bone metastases. Histology of prostate cancer metastases in mouse (Fig. 4) have shown small tumour cells infiltrating a less dense bone matrix and averaging of these two environments over the imaging voxel may account for the relatively low intracellular volume fraction ($f_{IC}$~0.36). Future work will test the ability of model parameters to stratify patients based on outcome.

**Table 3** Summary of parameter means (all pts) and $SD_{intratum}$ (across 5 slices, mean for 4 ROIs)

| | Ball | BB | | BBS | | | | |
|---|---|---|---|---|---|---|---|---|
| | $D_{p+EC+IC}$ ($mm^2$/s) | $f_p$ | $D_{EC+IC}$ ($mm^2$/s) | $f_p$ | $f_{IC}$ | $D_{EC}$ ($mm^2$/s) | $D_{IC}$ ($mm^2$/s) | R (µm) |
| Mean | 0.76 x $10^{-3}$ | 0.32 | 0.41 x $10^{-3}$ | 0.08 | 0.36 | 1.2 x $10^{-3}$ | 1.3 x $10^{-3}$ | 10. |
| $SD_{intratum}$ | 0.03 x $10^{-3}$ | 0.01 | 0.02 x $10^{-3}$ | 0.04 | 0.13 | 0.5 x $10^{-3}$ | 0.4 x $10^{-3}$ | 4 |

**REFERENCES**: 1. Scher, HI et al. 2011. *J Clin Oncology*, **29**: 3695. 2. Scher, HI et al. 2004. *J Clin Oncology*, **22**: 537. 3. Panagiotaki, E. et al. 2014. *Cancer Res*, **74**: 1902. 4. Panagiotaki, E. et al. 2015. *Invest Radiol*, In Press. 5. Akaike, H. 1974. *IEEE Trans Autom Control*, **19**: 716.